4. CONCLUSION

The primary objective of this experiment was to measure and evaluate the susceptibility of a C-band satellite DTV receiver to UWB interference. The secondary objective was to determine if DTV susceptibility could be predicted from measured signal characteristics. A final objective was to determine if continuous and gated Gaussian noise could be used to emulate DS and MB signals, respectively, in susceptibility tests. Each of these objectives are addressed in these concluding remarks.

4.1. Signal Sets of Common DTV Susceptibility Behavior

The primary objective of this experiment was to measure and evaluate the susceptibility of a DTV victim receiver to UWB interference. INR_{TOV} is our primary DTV susceptibility metric, i.e., DTV susceptibility increases as INR_{TOV} decreases and conversely decreases as INR_{TOV} increases. Table 10 provides ΔINR_{TOV} for the UWB signals ranked from least to most susceptible, where ΔINR_{TOV} is normalized to the INR_{TOV} of Gaussian noise. Notice that variation with *SNR* does not affect ranking, and for all signals except DP-01 *SNR* variation is minimal. Superimposed upon this ranking is categorization into three signal sets distinguished by their distance from the INR_{TOV} of Gaussian noise, i.e., Set 1 is defined as -0.5 dB $\leq \Delta INR_{TOV} \leq$ 0.5 dB, Set 2 is defined as $\Delta INR_{TOV} <$ -0.5 dB, and Set 3 is defined as $\Delta INR_{TOV} >$ 0.5 dB.

Table 10. Ranked DTV Susceptibility relative to Gaussian Noise Degradation

Rank	Signal	ΔINR_{TOV} (dB)			Set
		SNR = 9 dB	*SNR* = 12 dB	*SNR* = 15 dB	
1	DP-01	9.5	15.0	16.1	3
2	DP-03	0.3	0.4	0.5	1
3	MB-01	-0.1	0.2	0.3	
4	DS-03	0.2	0.3	-0.1	
5	DS-04	-0.1	0.3	0.1	
6	DS-05	-0.1	0.3	0.1	
7	DP-04	0.2	0.2	-0.2	
8	GN-01	0.0	0.0	0.0	
9	DS-01	-0.1	0.1	0.0	
10	DS-02	-0.2	0.2	-0.1	
11	DS-06	-0.5	-0.2	-0.3	
12	MB-02	-1.0	-1.0	-1.2	2
13	DP-02	-1.5	-1.2	-1.1	
14	MB-03	-1.4	-1.8	-2.0	
15	MB-04	-2.1	-2.4	-3.0	
16	MB-05	-3.7	-4.2	-5.0	
17	MB-07	-3.8	-4.5	-5.1	
18	MB-06	-5.6	-6.3	-6.6	
19	MB-08	-5.6	-6.5	-7.0	
20	MB-09	-8.4	-8.8	-9.4	

Signals in Set 1 are for all practical purposes equivalent to Gaussian noise in terms of DTV susceptibility. Signals in Set 2 have INR_{TOV} measurably below that of Gaussian noise and consequently are more deleterious to DTV reception. DP-01 is the only signal in Set 3; its INR_{TOV} is considerably greater than that of Gaussian noise and therefore is the most benign to DTV reception. Demarcation of Sets 1 and 3 is relatively straightforward as they are separated by a wide margin. Demarcation of Sets 1 and 2, however, is slightly more subjective. For example, INR_{TOV} of MB-02 is merely 1.0 – 1.2 dB below that of Gaussian noise.

During this experiment, there was interest in understanding the effects of UWB interference on the DTV forward error correction, consisting of a Viterbi decoder, convolutional byte de-interleaver, and Reed-Solomon decoder. Having access only to pre-Viterbi *BER* and post-Reed-Solomon *SER*, the FEC was regarded as a black box whose performance was evaluated by the average number of bit errors it corrected. In particular, FEC performance was deemed good when it achieved $SER_{TOV} = 10^{-4}$ from a relatively high BER_{TOV}. Interestingly in Sets 1 and 2, poor FEC performance, i.e., low BER_{TOV}, was correlated with high DTV susceptibility, i.e., low INR_{TOV}. Inspection of MB-01 and MB-09 in Table 7 (*SNR* = 12 dB), for example, shows that BER_{TOV} decreased from 0.041 to 0.006 as INR_{TOV} decreased from 5.6 dB to -3.4 dB. As was pointed out in Section 2.2.2, DP-01 in Set 3 did not correlate in the same way. Disregarding this exception, the correlation between BER_{TOV} and INR_{TOV} indicates that FEC plays a strong role in susceptibility. The effects of UWB interference on FEC performance is a topic for further study.

4.2. Summary of Measured Signal Characteristics

UWB signal characterization measurements were performed in the DTV victim signal bandwidth. Measured UWB signals were subjected to temporal, amplitude, and spectral analyses. Temporal analyses used *BD* and *BI* statistics and corresponding ζ_{DTV} estimates. Amplitude analyses used the *APD* and *P/A*. Finally, spectral analyses focused on the *PSD*.

Temporal analyses of DP and DS signals showed that band-limiting elongated pulse width, w. This was evident in Table 4, which demonstrates that $BD > w$ and $\zeta_{DTV} > \zeta$. For signals with T_{pulse} less than or comparable to $1/B_{DTV}$, elongated pulses overlapped and the subsequent *APD* and *P/A* approached Rayleigh amplitude statistics. For signals with T_{pulse} significantly greater than $1/B_{DTV}$, elongated pulses remained distinct and a step-like *APD* occurred with correspondingly high *P/A*.

Similar results were observed with the MB signals; in these cases, however, band-limiting elongated on-time, τ_{on}, and shortened off-time, τ_{off}. These changes were evident in Table 8, which demonstrated $BD > \tau_{on}$, $BI < \tau_{off}$, and $\zeta_{DTV} > \zeta$. For signals with τ_{off} less than or comparable to $1/B_{DTV}$, elongated on-times overlapped and the subsequent *APD* and *P/A* approached Rayleigh amplitude statistics. For signals with τ_{off} significantly greater than $1/B_{DTV}$, elongated on-times remained distinct and a step-like *APD* occurred with correspondingly high *P/A*.

Spectral analyses of DP, DS, and MB signals revealed flat power spectral densities like white Gaussian noise. A notable exception to this was DS-06 whose *PSD* sloped several dB over the DTV signal bandwidth. Theoretical analysis demonstrated that this was due to the DS code word spectral characteristics. Further comments on spectral analyses for bandwidths other than B_{DTV} can be found in Section 4.4.

4.3. Correlations Between DTV Susceptibility and Signal Characteristics

The second objective of this experiment was to determine if DTV susceptibility could be predicted from measured signal characteristics. Indeed, in Part 2 of this report series it was found that DTV susceptibility to gated noise interference could not be predicted by interference power alone. It was demonstrated that DTV susceptibility was also dependent on the temporal parameters of the gated noise signals, i.e., τ_{on}, τ_{off}, and ζ. In this section, the analysis is taken one step further by plotting DTV susceptibility versus the band-limited metrics *BD*, *BI*, ζ_{DTV}, and *P/A*.

Figures 38 and 39 summarize the temporal metrics of the UWB signals and illustrate how DTV susceptibility, i.e., ΔINR_{TOV}, depends on these metrics. Figure 38 provides *BI* versus *BD* of the UWB signals, and Figure 39 provides ΔINR_{TOV} as a function of ζ_{DTV}. In both plots, contours are drawn around the DTV susceptibility sets identified in Section 4.1. Signals within Set 1 have short $BI < 1/B_{DTV}$ and a wide range of longer *BD*. For these signals, the pulse period or gating off-time is less than $1/B_{DTV}$, and band-limiting caused overlapping. This either preserved or created signal characteristics that resembled continuous noise as evidenced by ζ_{DTV} near unity. Hence, INR_{TOV} for signals within Set 1 resembles that of Gaussian noise. Signals within Set 2 have a wide range of $BI > 1/B_{DTV}$ and *BD*. For these signals, the pulse period or gating off-time is greater than or comparable to $1/B_{DTV}$, and band-limiting did not create a continuous interference signal as evidenced by ζ_{DTV} ranging from 0.05 to 0.4. The wide range of *BD* and *BI* for signals within Set 2 caused a correspondingly wide range of ΔINR_{TOV} below that of Gaussian noise, where the DTV receiver was most susceptible to signals with long *BD* and *BI*, e.g., MB-09, and least susceptible to signals with short *BD* and *BI*, e.g., MB-02 and DP-02. DP-01 in Set 3 has long $BI >> 1/B_{DTV}$. For this signal, *BD* is much less than *BI* making ζ_{DTV} small. Hence, the victim receiver was exposed to interference the least amount of time, and ΔINR_{TOV} is significantly greater than that of Gaussian noise.

Contours drawn around signals within the DTV susceptibility sets, defined by ΔINR_{TOV} alone, persist as regions when plotted against the temporal metrics *BD*, *BI*, and ζ_{DTV}. These findings suggest that DTV susceptibility categorization can be predicted from a priori knowledge of these band-limited metrics. Results suggest that UWB signals with ζ_{DTV} close to unity will generate interference much like Gaussian noise. Further, results suggest that UWB signals with ζ_{DTV} approaching zero will generate benign interference. Finally, results suggest that UWB signals with $0.05 \leq \zeta_{DTV} \leq 0.4$ are likely to generate a range of interference effects more deleterious than Gaussian noise interference, which requires more knowledge to determine the specific impact on the victim receiver. For example, Figure 39 shows the signals clustering horizontally with those having the same number of bands. Within these clusters, signals are differentiated vertically by their dwell. Understanding this dependence on dwell required the in-depth study of the effects of gated noise on-time given in Part 2 of this report series.

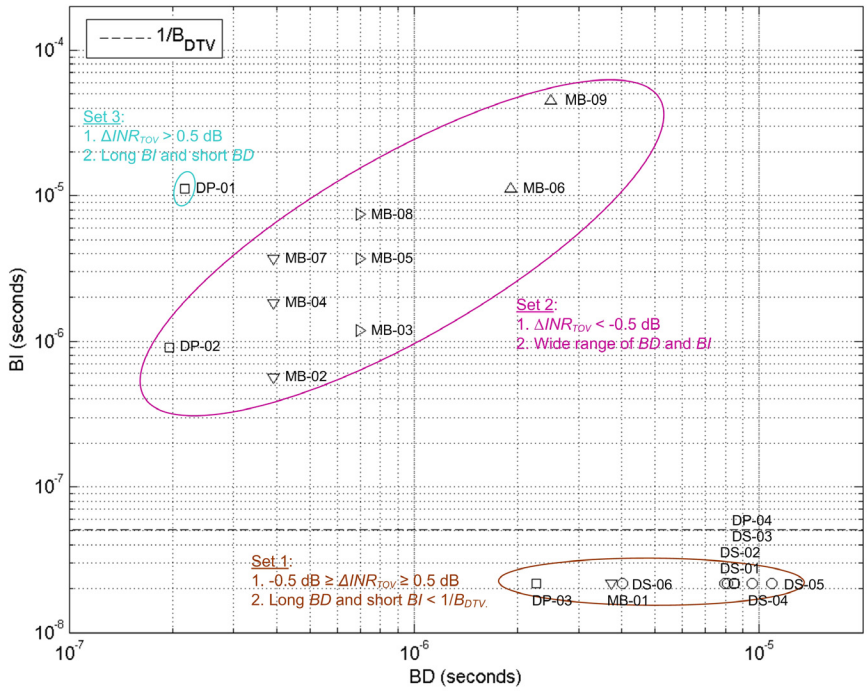

Figure 38. *BI* versus *BD* of UWB interference. Contours are drawn around signals within the same DTV susceptibility set.

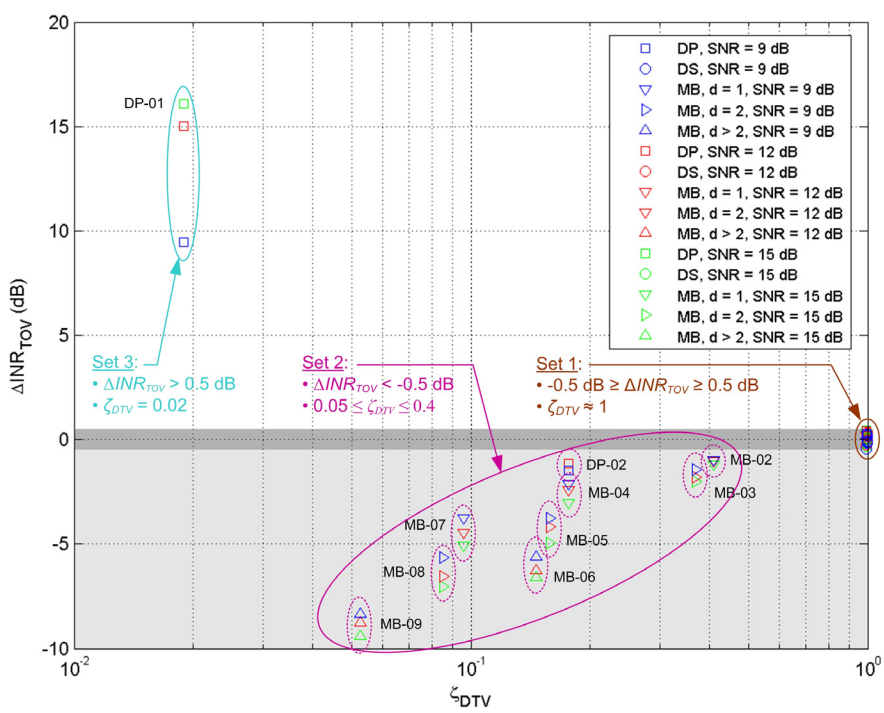

Figure 39. ΔINR_{TOV} versus ζ_{DTV} of UWB interference. Contours are drawn around signals within the same DTV susceptibility set.

Figure 40 provides ΔINR_{TOV} versus P/A with contours drawn around the DTV susceptibility sets. Signals within Set 1 are in a horizontal line in the range 5.4 dB $\leq$ P/A $\leq$ 9.6 dB, which indicates that the peaks of these signals have negligible effect on ΔINR_{TOV}. Signals within Set 2 follow a downward trend in the range 12.8 dB $\leq$ P/A $\leq$ 18.9 dB, which indicates that DTV susceptibility increases with increasing P/A. Exact determination of the P/A transitions between Sets 1 and 2 and Sets 2 and 3 requires further investigation.

Contours drawn around the signals within the DTV susceptibility signal sets, defined by ΔINR_{TOV} alone, persist as regions when plotted against P/A. This suggests that DTV susceptibility categorization can be predicted from a priori knowledge of the P/A metric. Results suggest that UWB signals with 5.4 dB $\leq$ P/A $\leq$ 9.6 dB will generate interference much like Gaussian noise. Further, results suggest that UWB signals with exceedingly high P/A will generate benign interference. Finally, results suggest that UWB signals with 12.8 dB $\leq$ P/A $\leq$ 18.9 dB are likely to generate a range of interference effects more deleterious than Gaussian noise interference, which requires more knowledge to determine the specific impact on the victim receiver.

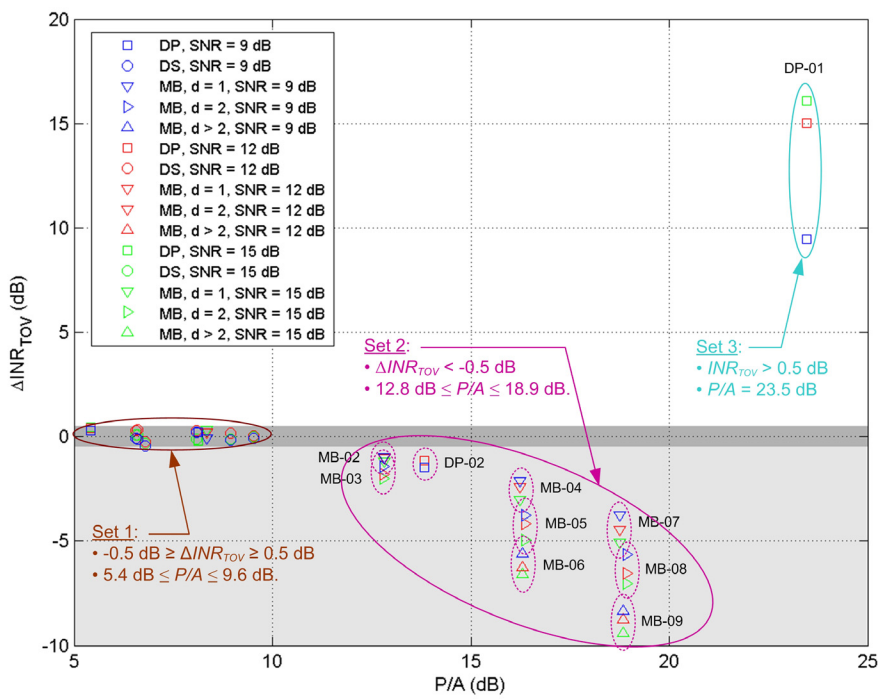

Figure 40. ΔINR_{TOV} versus P/A of UWB interference. Contours are drawn around signals within the same DTV susceptibility set.

In Section 4.1, it was mentioned that ΔINR_{TOV} varied slightly with SNR in Sets 1 and 2. This variation manifests itself as vertical displacement of ΔINR_{TOV} with SNR in Figures 39 and 40. Displacement of BD, BI, ζ_{DTV}, and P/A with SNR are not applicable since these metrics were derived from RF measurements. Hence, horizontal displacement of BD and vertical displacement of BI in Figure 38, horizontal displacement of ζ_{DTV} in Figure 39, and horizontal displacement of P/A in Figure 40 do not exist.

4.4. UWB Signal Emulation

As stated previously, the last objective of this study was to determine whether continuous and gated noise could be used to emulate DS and MB signals, respectively, in these and other susceptibility tests. This objective is important since gated noise is easier to implement and analyze than the UWB signals.

The main body of this report provided temporal, amplitude, and spectral analyses for each of the signals band-limited to B_{DTV}. With two exceptions, these analyses demonstrated that DS signals are similar to Gaussian noise. First, *P/A*s of the DS signals were 0 – 3 dB less than *P/A* of Gaussian noise. Consequently, *APD*s of the DS signals deviated slightly from Rayleigh. Second, the *PSD* of DS-06 sloped several dB over the DTV signal bandwidth in contrast to the flat spectrum of white Gaussian noise. This slope was attributed to the spectrum of the direct sequence codeword. Similarly, these analyses showed that gated noise was similar to MB signals with the exception that the *P/A* was 1 – 2 dB less than those of GN(MB).

The similarities were also present in the DTV susceptibility results, which were nearly identical for comparative signals. Hence, it appears reasonable to substitute continuous and gated noise signals for DS and MB signals, respectively, when replicating this experiment.

APD statistics as a function of frequency in Section B.4, however, suggest that GN(MB) signals cannot be used in place of MB signals for susceptibility tests on victim receivers with narrower bandwidths. These statistics show significant variation as a function of frequency when the signal is band-limited to 1.0 and 0.1 MHz. *APD* statistics versus frequency in the 1-MHz bandwidth case have a distinct periodic lobing pattern. *APD* statistics versus frequency in the 0.1-MHz bandwidth case have a distinct periodic spiking pattern centered at the pilot tone frequency. These features are not present in the GN(MB) signals and require further analysis.